

Theoretical Study of Laser Produced Platinum Plasma

¹Wissam Hasan Mahdi, ²Nawal Murad Muhammad

Department of Physics, College of Education for Girls, University of Kufa, Najaf, Iraq.

Abstract: A theoretical study of the laser produced platinum (Pt) plasma was carried out using hydrodynamic simulation program MED103. A CO₂ laser with wavelength of 10.6 μm was focused on platinum Z=78, to evaluate the spatial temporal development of hydrodynamic properties of plasma. The electron temperature, electron density and average charge were simulated with changing laser intensity and laser pulse width. The laser pulse duration of 20 ns was more suitable to produce emission in water window spectral region it generate higher electron temperature with lower laser intensity.

Keywords: laser produced plasma (LPP), EUV, X-rays, The platinum plasma, CO₂ laser, MED103.

1. INTRODUCTION

The basic principle of laser produced plasma (LPP) in simple way is that a high intensity laser pulse is fired at a target material of some sort and by absorbing the laser energy a hot plasma is created that emits extreme ultraviolet (EUV) and X-rays [1]. The shorter wavelength source emitted from hot plasma of high-Z element has been taken a wide range of researchers' interest because of their numerous applications [2]. The wavelengths in EUV and soft X-ray regions has been employed in science and technology such as lithography [3]. Three dimensional imaging [4] x-ray microscopy [5] and microscope of biological structure. The laser produced high Z plasma generates high power EUV source at 13.5 nm [6-7] and 6.7 nm [8] for semiconductor lithography based on strong emission of 4d-4f and 4p-4d transition which overlaps in the adjacent ion stage of Sn (Z=50) and Gd (Z=64) respectively [9]. The plasma of higher atomic number elements produce a shorter wavelength from a UTA unresolved transition array of n=4-n=4 and n=4-n=5 [10]. These emissions are expected to lie in (2-4) nm water windows if Z=78 (Pt) to Z=83 (Bi) [11]. The platinum element, as a solid target, is one of the elements that form laser-produced plasma in the soft X-ray region at the water window for microscopic visualization of live cells. The emissions in the water window region (1.9-4.2) nm originate from the overlapping of the 4f-5g transitions, and the peaks corresponding to the different ionization phases are separate and clear. The ions that participate in emissions in the

spectral region at the water window start from the Pt⁺¹⁹ ion to the Pt⁺³¹ ion, and the greatest emission results from the Pt⁺²⁴ ion [12]. To expose the picture of the biological sample on the detector during x-ray microscopy, the photon flow from the x-ray source must be adequate. Synchrotrons and, more recently, free electron lasers (FEL) are the most efficient ways to create high-power, high-brightness x-rays [13]. In a typical setup, the sample is illuminated by an X-ray source that uses a condenser. A high-resolution objective is a micro-zone plate. A CCD detector's expanded picture is read out using thin back illumination. An X-ray microscope's resolution may be limited to the zone plate's outermost zone width [14]. Zone plates with zone widths as small as 15 nm have recently been developed [15]

2-RESULTS

The hydrodynamic simulation program MED103 was used to evaluate the hydrodynamic parameter of platinum plasma produced by CO₂ laser with energies of (3,4,5,6 and 7) J for pulse duration of 15 ns and 20 ns (FWHM). The CO₂ laser focusing spot with a diameter of 20 μm was an incident perpendicular on to the cylindrical platinum target. The laser intensity was in the range of (1.19 – 3.71) W/cm². The one dimension evolution of electron temperature, average charge and electron density were recorded in space and time within 100 ns simulation time. The value of maximum electron temperature was determined, in addition the electron density and average charge at the same position and time of maximum Te were recorded.

At a pulse duration of 15 ns 2-1

The maximum electron temperature in Pt plasma is direct propotional with laser intensity as shown in table 1. The average ion stages also increses with increasing of electron temperature and laser

intensity. It is in the range of 28 to 38.9 that is suitable for producing water window emission. The thin plasma where the electron density around 10^{19} cm^{-3} reduces self-absorption so more efficient for water window radiation.

Table (1) values of the maximum temperature of electrons T_e , ion average Z^* and electron density n_e at a pulse time of 15ns and for different laser energies.

Laser energy (J)	Laser intensity (Wcm^{-2}) $\times 10^{13}$	T_e (ev)	Z^*	Log n_e (cm^{-3})	Time (ns)	Distance (μm)
3	1.5915	179.06	28	19.4287	25.0036	317.26
4	2.1221	245.17	33.066	18.846	33.0152	550.27
5	2.6526	331.91	35.497	18.8267	32.0287	552.31
6	3.1831	436.37	37.515	18.8158	31.0217	544.63
7	3.7136	517.92	38.9	18.8343	30.0328	526.62

exceeds 40, Figure (1(b)) the temperature of electrons whose greatest value is more than 500 eV after a period of formation platinum plasma. Figure (1(c)) shows the electron density .

Figure (1) shows the laser-produced platinum plasma using a laser energy of 7 J, a pulse time of 15 ns, and a power density of ($3.7136 \times 10^{13} \text{ Wcm}^{-2}$). Figure (1 (a)) shows the rate of Z^* ions that

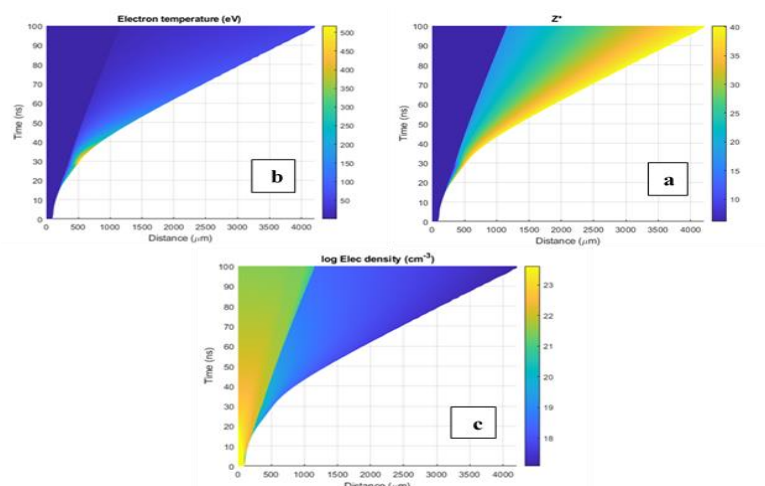


Figure (1) Change of the laser-produced platinum plasma with respect to time and distance at 7J energy and 15ns pulse duratio 15ns (a) Change the average of ions with respect to time and distance (b) Change the temperature of electrons with respect to time and distance (c) Change the density of electrons with respect to time and distance .

At a pulse duration of 20 ns 2-2

Table 2 calculated the maximum temperature of electrons, average of ions and density of electrons temporally and spatially at the different energies

Table (2) values of the maximum electron temperature T_e , ion average Z^* and electron density n_e at a pulse time of 20 ns and for different laser energies.

Laser energy (J)	Laser intensity (Wcm^{-2}) $\times 10^{13}$	T_e (ev)	Z^*	Log n_e (cm^{-3})	Time (ns)	Distance (μm)
3	1.1937	254.98	30.554	18.792	42.0024	617.99
4	1.5915	364.69	33.632	18.7969	40.0324	617.44
5	1.9894	485.85	35.903	18.8104	38.0332	602.42
6	2.3873	600.9	37.833	18.7983	37.052	601.833
7	2.7852	701.96	39.149	18.7967	36.0391	595.25

and pulse duration 20 ns . It was found that at a laser energy 3J produces an average of ions within limits 30 , which is very suitable for emissions in the X-ray region the water window[16].

Figure (2) shows the laser-produced platinum plasma using a laser energy of 7 J, a pulse time of 20 ns, and a laser power density ($2.7852 \times 10^{13} \text{ Wcm}^{-2}$). Figure (2(a)) shows the average of ions that reach more than 40 at their maximum value.

Figure (2(b)) The temperature of electrons that reaches more than 700 ev after a period of platinum plasma formation. Figure (2(c)) shows the density of electrons.

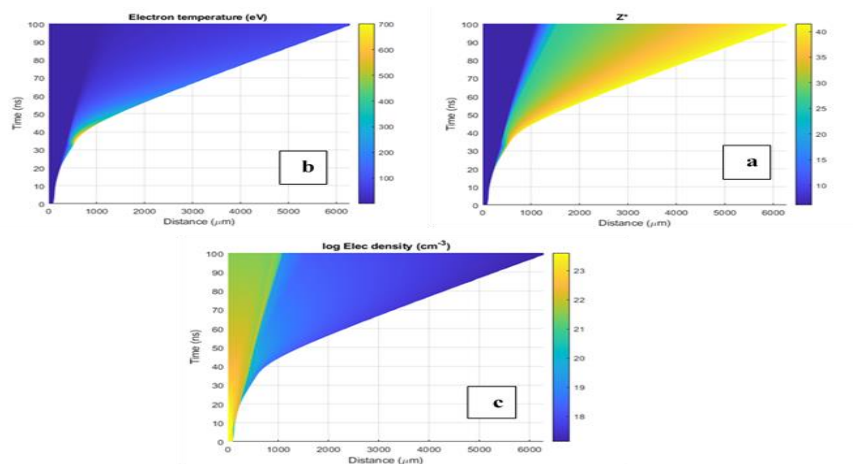


Figure (2) Change of laser-produced platinum plasma parameters with respect to time and distance at 7 J energy and pulse duration of 20 ns of laser pulse time and laser power density on plasma parameters
Effect2-3

- (a) Change of ion average with respect to time and distance
- (b) Change of electron temperature with respect to time and distance
- (c) Electron density change with respect to time and distance.

Using two laser pulse times 15 ns and 20 ns, we observe that with increasing laser power, the maximum electron temperature will gradually increase as a function of power density. At the laser pulse duration of 20 ns, the temperature of the electrons is greater than it at 15 ns so when the laser pulse increases, the plasma will be hotter because there is enough time for plasma to absorb more photon from laser. This behavior is illustrated in Figure (3).

It was noted that the results obtained at a pulse duration of 20 ns are better than the results at a duration of a pulse of 15 ns. At a laser energy of 6 J, the maximum electron temperature was 600 eV, which is very suitable for ionizing the atoms of the platinum element to participate in the spectral emission at the water window[17].

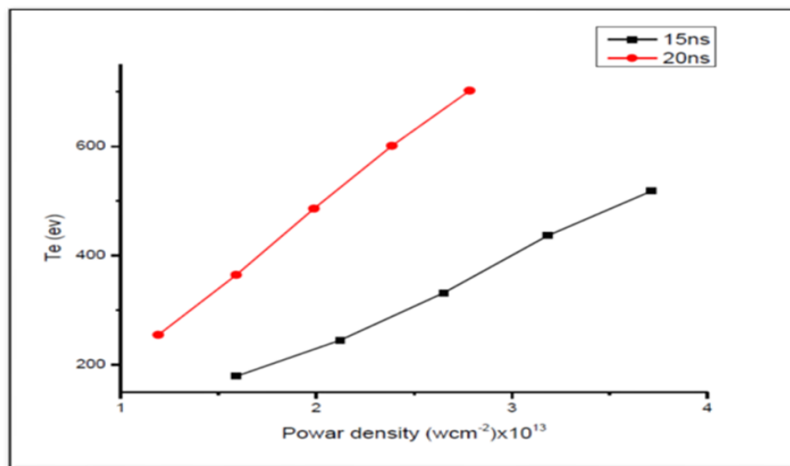


Figure (3) The maximum electron temperature of the laser-produced platinum plasma as a function The intensity of the laser for different the laser pulse duration.

Figure (4) shows the behavior of changing the value of the ion average Z^* as a function of the laser power density at a range of energies and for two times only. At a laser pulse time of 15 ns and a laser energy of 3J, the rate of ions is 28, then it begins to increase until it reaches 38 at a laser energy of 7J As for a pulse time of 20 ns and a laser

energy value of 3J, the rate of ions Z^* is about 30 and increases with increasing energy, reaching 39 at a laser energy of 7J. That is, the rate of ions increases with the increase of the laser energy as well as with the increase in the temperature of the electrons.

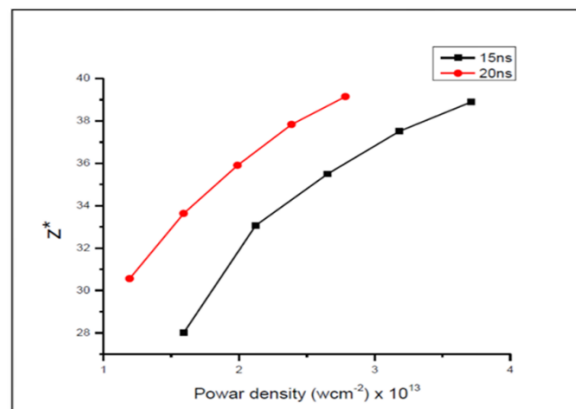


Figure (4) The change in the average of ions Z^* as a function of the laser power density during different energies and two times at the highest temperature of the electrons

Figure (5) shows the behavior of the electron density, where there is no effect of the pulse duration, and the results are close for time and location as a function of intensity.

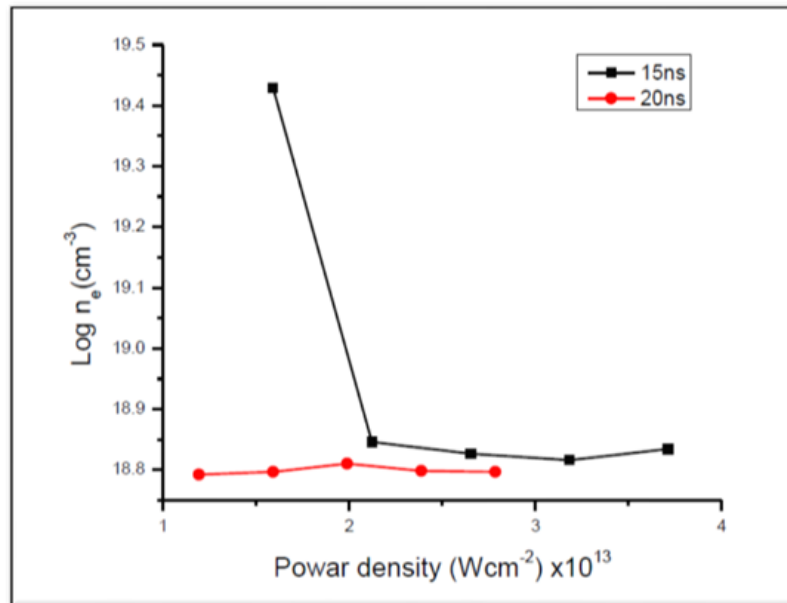


Figure (5) The change of electron density at the highest temperature as a function of the laser power density at different laser pulse times.

3. CONCLUSION

The simulation of laser produced platinum plasma in one dimension shows that the high electron temperature constrained in small area within and after laser pulse duration while the high average ion cover wide plasma area along simulation time. The maximum electron temperature and average charge are proportional to laser intensity and laser pulse duration, while the electron density at maximum electron temperature still around of 10^{19} cm^{-3} even with changing laser intensity and pulse duration so, the plasma can be considered thin plasma that reduced self absorption and more efficient emission in the water window spectral region.

ACKNOWLEDGMENTS

The authors are thank to Padraig Dunne and spectroscopy group at UCD for permission to use and giving us MED103 code. They would also like to thank the University of Kufa, the Ministry of Higher Education and Scientific Research, Iraq, for their support as part of this work. They would also like to thank the Department of Physics, College of Education for Girls.

REFERENCE

- [1] G. O'Sullivan, A. Cummings, C. Z. Dong, P. Dunne, P. Hayden, O'Morris, E. Sokell, F. O'Reilly, M. G. Su and J. White, "Emission and absorption in laser produced plasmas: processes and applications", J. Phys.: Conf. Ser. 163, 012003, (2009).
- [2] J. A. van Bokhoven, C. Lamberti, "X-Ray Absorption and X-Ray Emission Spectroscopy" Theory and Applications (John Wiley & Sons, 2016).
- [3] T. Otsuka, D. Kilbane, J. White, T. Higashiguchi, N. Yugami T. Yatagai, W. Jiang, A. Endo, P. Dunne, and G. O'Sullivan, "Rare-earth plasma extreme ultraviolet sources at 6.5–6.7 nm", Appl. Phys. Lett. 97, 111503, (2010).
- [4] P. A. C. Jansson, U. Vogt, and H. M. Hertz, "Liquid-nitrogen-jet laser-plasma source for compact soft X-ray microscopy", Rev. Sci. Instrum. 76, 043503, (2005).
- [5] M. Bertilson, O. von Hofsten, U. Vogt, A. Holmberg, and H. M. Hertz, "High-resolution computed tomography with a compact soft X-ray microscope", Opt. Express 17, 11057, (2009).

- [6] T. Wu, T. Higashiguchi, B. Li, Y. Suzuki, G. Arai, T. Dinh, P. Dunne, F. O'Reilly, E. Sokell and G. O'Sullivan, "*XUV spectral analysis of ns- and ps-laser produced platinum plasmas*" *Journal of Physics B: Atomic, Molecular and Optical Physics*, 48 ,245007 (10pp) (2015).
- [7] J. C. Solem and G. C. Baldwin, *Science "Microholography of Living Organisms"*, 218, 229 (1982).
- [8] V. Bakshi, "*EUV Source for Lithography*", SPIE, Bellingham, WA, USA, (2006).
- [9] T. Higashiguchi, B. Li, Y. Suzuki, M. Kawasaki, H. Ohashi, S. Torii, D. Nakamura, A. Takahashi, T. Okada, W. Jiang, T. Miura, A. Endo, P. Dunne, G. O'Sullivan, and T. Makimura, "***Characteristics of extreme ultraviolet emission from mid-infrared laser-produced rare-earth Gd plasmas***" *Optical Society of America* (2013).
- [10] C.S. Harte, T. Higashiguchi, T. Otsuka, R. D'Arcy, D. Kilbane and G. O'Sullivan, "***Analysis of tungsten laser produced plasmas in the extreme ultraviolet (EUV) spectral region***" *J. Phys. B: At. Mol. Opt. Phys.* 45 205002 (6pp) (2012).
- [11] T.H. Dinh, Y. Suzuki, G. Arai, B. Li, P. Dunne, G. O'Sullivan, S. Fujioka, N. Hasegawa, T. Kawachi, M. Nishikino, and T. Higashiguchi, "***Temporal behavior of unresolved transition array emission in water window soft x-ray spectral region from multiply charged ions***" *Appl. Phys. Lett.* 107, 121101 (2015).
- [12] C. Wagner and N. Harned, "*Lithography gets extreme*", *Nat. Photonics* 4, 24, (2010).
- [13] T. Gorniak, R. Heine, A. P. Mancuso, F. Staier, C. Christophis, M. E. Pettitt, A. Sakdinawat, R. Treusch, N. Guerassimova, J. Feldhaus et al., *Opt. Express.* "*X-ray holographic microscopy with zone plates applied to biological samples in the water window using 3rd harmonic radiation from the free-electron laser FLASH*", 19, 11059 (2011).
- [14] Rarback, H., Kenny, J., Kirz, J. & Xie, X. "*Scanning X-ray Microscopy-First Tests with Synchrotron Radiation*", *Scanned Image Microscopy*, pp. 449–456. Academic Press, London. (1980).
- [15] Attwood, D.T. "*Soft X-Rays and Extreme Ultraviolet Radiation*", Cambridge University Press, Cambridge (1999).
- [16] T. Wu, T. Higashiguchi, B. Li, Y. Suzuki, G. Arai, T. Dinh, P. Dunne, F. O'Reilly, E. Sokell and G. O'Sullivan, "***XUV spectral analysis of ns- and ps-laser produced platinum plasmas***" *Journal of Physics B: Atomic, Molecular and Optical Physics*, 48 ,245007 (10pp) (2015) .
- [17] H. Hara, G. Arai, Y. Kondo, T.H. Dinh, P. Dunne, G. O'Sullivan, T. Ejima, T. Hatano, W. Jiang, M. Nishikino, A. Sasaki, A. Sunahara, and T. Higashiguchi, "***Characteristics of the soft X-ray emission from laser-produced highly charged platinum plasmas***" *Applied Physics Express* 9, 066201 (2016).